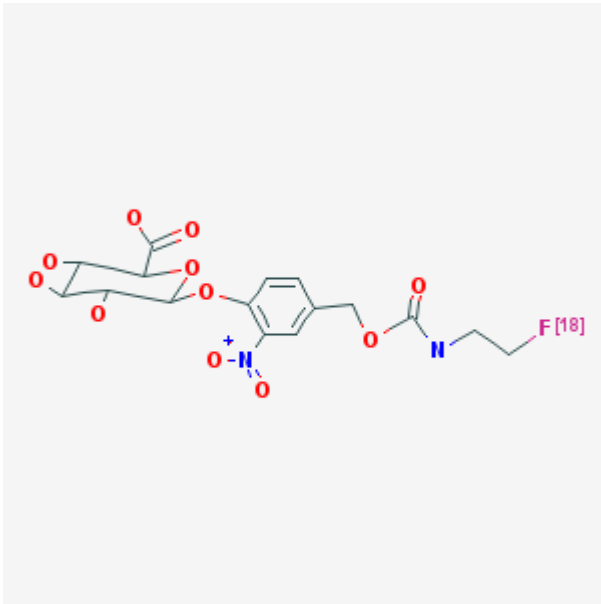


1-O-(4-(2-[¹⁸F]Fluoroethyl-carbamoyloxymethyl)-2-nitrophenyl)-O-β-D-glucopyronurate

[¹⁸F]FEAnGA

Arvind Chopra, PhD¹

Created: March 28, 2012; Updated: April 27, 2012.

Chemical name:	1-O-(4-(2-[¹⁸ F]Fluoroethyl-carbamoyloxymethyl)-2-nitrophenyl)-O-β-D-glucopyronurate	
Abbreviated name:	[¹⁸ F]FEAnGA	
Synonym:		
Agent Category:	Compound	
Target:	β-Glucuronidase (β-GUS; βG)	
Target Category:	Enzyme	
Method of detection:	Positron emission tomography (PET)	
Source of signal / contrast:	¹⁸ F	
Activation:	Yes	
Studies:	<ul style="list-style-type: none"> • <i>In vitro</i> • Rodents 	

Click on above structure for more information in [PubChem](#).

¹ National Center for Biotechnology Information, NLM, Bethesda, MD 20894; Email: micad@ncbi.nlm.nih.gov.

NLM Citation: Chopra A. 1-O-(4-(2-[¹⁸F]Fluoroethyl-carbamoyloxymethyl)-2-nitrophenyl)-O-β-D-glucopyronurate. 2012 Mar 28 [Updated 2012 Apr 27]. In: Molecular Imaging and Contrast Agent Database (MICAD) [Internet]. Bethesda (MD): National Center for Biotechnology Information (US); 2004-2013.

Background

[PubMed]

The β -glucuronidase (β -GUS; EC 3.2.1.31) is a lysosomal enzyme that is known to activate prodrugs (PDs) for the treatment of cancer. β -GUS has been used to track the path of gene delivery vehicles, and there is evidence that it can be used as a tumor marker (1). The primary function of the enzyme is to catalyze the hydrolysis of β -glucuronic acid residues from the cell-surface glycosaminoglycans for normal restructuring of the extracellular matrix (ECM) (2), and the enzyme is believed to participate in the processes of angiogenesis, cancer metastasis, and inflammation (3). Normal tissues have low levels of β -GUS in the ECM, but tissues under pathological stress, such as bacterial infection, fibrosis, and malignancy, show elevated levels of the enzyme (4). Intracellular β -GUS is released from necrotic cells, and its activity in these lesions has been used to activate anti-cancer PDs *in situ* to treat cancers (2). Chemotherapeutic anti-cancer drugs are generally nonselective and toxic to healthy cells; thus, they are of limited efficacy to the patient due to their side effects. The conversion of a toxic drug into a non-toxic PD that can be activated only under specific conditions (e.g., enzyme catalysis or chemical hydrolysis) would facilitate drug activation only in tissues that provide the specialized microenvironment and improve its concentration and efficacy at the desired location in the body (5, 6). For example, glucuronide PDs (drugs that are linked to a glucuronic acid moiety with or without a linker) have been shown to have superior anti-tumor activity compared with the parent drugs because the activated drugs are released from the PDs by the β -GUS activity in a site-specific manner (7, 8).

β -GUS activity varies among individuals, and its expression or accumulation in tumor tissues may change depending on the location in the body or the type of neoplasm (2, 9). Fluorescent or bioluminescent substrates were developed to determine the expression of β -GUS with optical imaging in various tissues of mice (1). However, this imaging modality is suitable for the detection of fluorescence or bioluminescence signals generated only in the superficial tissues of small animals such as rodents; the low depth of light penetration in tissues is a limitation for its application in large animals and humans (2, 4, 10). Imaging modalities such as positron emission tomography (PET) and single-photon emission computed tomography (SPECT), which use radionuclides to generate tracer signals, can be used to detect and determine the activity of enzymes such as the β -GUS because signals generated by radiolabeled probes can be detected even in deep tissues of the body (11). In general, PET imaging has a higher sensitivity than SPECT and has been used to investigate drug kinetics in preclinical and clinical settings (11). A ^{124}I -labeled phenolphthalein glucuronide PD probe (^{124}I -PTH-G) was developed and evaluated with microPET for the detection of xenograft tumors that express β -GUS in mice (9). Although ^{124}I -PTH-G was suitable for the detection of tumors in the rodents, biodistribution studies of the tracer in these animals revealed that, even at 20 h postinjection (p.i.), higher levels of the label could be detected in the liver, gallbladder,

stomach, and intestines than in the tumors. Therefore, the investigators concluded that [¹²⁴I]-PTH-G is probably unsuitable for the imaging of tumors that express β-GUS.

Antunes et al. synthesized 1-*O*-(4-(2-[¹⁸F]fluoroethyl-carbamoyloxymethyl)-2-nitrophenyl)-*O*-β-*D*-glucopyronuronate ([¹⁸F]-FEAnGA) as a PD in an effort to develop a probe that could be used with PET to detect and visualize β-GUS activity in tissues (4). The mechanism of *in vitro* or *in vivo* activation of [¹⁸F]-FEAnGA is described elsewhere (4). Briefly, the hydrolysis of [¹⁸F]-FEAnGA by β-GUS results in the production of glucuronic acid, 4-hydroxy-3-nitrobenzyl alcohol (HNBA; this is the spacer in the intact FEAnGA molecule, and the concentration of HNBA in the reaction mixture can be measured with ultraviolet (UV) spectroscopy at 402 nm after the FEAnGA has been hydrolysed), and 2-[¹⁸F]fluoroethylamine ([¹⁸F]-FEA). [¹⁸F]-FEA subsequently accumulates in the cells (attributed to passive diffusion into the cells) and is detected with PET imaging. [¹⁸F]-FEAnGA has been evaluated for the detection of tumors that expressed β-GUS (2, 4) and inflammation (2, 10) in mice.

Related Resource Links

Other prodrug chapters in [MICAD](#)

[Homo sapiens β-GUS protein and mRNA sequences](#)

Prodrug-related [clinical trials](#)

Synthesis

[\[PubMed\]](#)

The synthesis of FEAnGA and its labeling with [¹⁸F]-fluoride have been described by Antunes et al. (4). The radiochemical yield (RCY) and radiochemical purity (RCP) of the labeled compound were reported to be 5%–20% (decay-corrected based on [¹⁸F]-fluoride) and 95%, respectively. The total time required for the synthesis and purification of the final labeled product was 150 min, and the specific activity of [¹⁸F]-FEAnGA was 5–10 GBq (135–270 μC)/μmol.

[¹⁸F]-FEA was synthesized for use in studies (4). The RCY of this radiochemical was 48 ± 9%. The RCP, specific activity, and stability of [¹⁸F]-FEA were not reported.

In Vitro Studies: Testing in Cells and Tissues

[\[PubMed\]](#)

[¹⁸F]-FEAnGA was stable in phosphate-buffered saline (pH not reported) and rat plasma at 37°C for at least 1 h and 3 h, respectively, as determined with radio-thin-layer chromatography (radio-TLC) (4).

The lipophilicity (Log *D*) of [¹⁸F]-FEAnGA in an *n*-octanol/water mixture was determined to be -1.01 ± 0.03 and -1.61 ± 0.01 at pH 3 and pH 7.4, respectively (4). The

lipophilicity of [^{18}F]-FEA at pH 7.4 was determined to be -0.69 ± 0.02 . This indicated that [^{18}F]-FEAnGA was ~ 10 -fold more hydrophilic than [^{18}F]-FEA due to the presence of a glucuronic acid moiety in its structure (4).

The enzyme kinetics parameters for nonradioactive FEAnGA with *Escherichia coli* β -GUS and bovine liver β -GUS are presented in Table 1 and will not be discussed here.

Table 1: *E. coli* β -GUS and bovine liver β -GUS enzyme kinetic parameters with FEAnGA (4)

β -GUS Enzyme	Substrate	K_M (μM)	V_{max} ($\mu\text{mol}/\text{min}$ per mg)	k_{cat} (s^{-1})	$\frac{k_{\text{cat}}}{K_M}$ ($10^6/\text{M}^{-1} \text{s}^{-1}$)
<i>E. coli</i>	PNPG	8.2 ± 1.6	$1,366 \pm 68$	660	80.3
	FEAnGA	7.1 ± 0.9	348 ± 24	134	24.6
Bovine liver β -GUS	PNPG	34.0 ± 16.5	56.9 ± 23	19	0.6
	FEAnGA	5.7 ± 2.7	25.8 ± 9	10	1.8

PNPG, *p*-nitro-phenyl- β -D-glucuronide, a reference substrate for β -GUS; K_M , Michaelis constant;

V_{max} , velocity of the reaction; k_{cat} , determines the catalytic formation of product under optimal reaction

conditions; k_{cat}/K_M , measure of the enzyme efficiency.

When C6 rat glioma cells were incubated with [^{18}F]-FEAnGA in the presence of either *E. coli* β -GUS or bovine liver β -GUS (in growth medium containing 10% fetal bovine serum), 4- and 1.5-fold higher amounts of radioactivity were observed to be associated with the cells, respectively, compared with controls (4). In addition, when C6 cells were incubated with [^{18}F]-FEA alone the amount of radioactivity associated with the cells was ~ 6 -fold higher than the radioactivity associated with cells exposed to [^{18}F]-FEAnGA without the β -GUS enzymes. The investigators ascribed the high uptake of radioactivity from [^{18}F]-FEA by the C6 cells to passive diffusion of the label across the cell membrane (4). Under these incubation conditions, 99% and 37% of [^{18}F]-FEAnGA was converted to [^{18}F]-FEA by the *E. coli* β -GUS and bovine liver β -GUS enzymes, respectively, as determined with radio-TLC of the cell growth medium.

The uptake of radioactivity from [^{18}F]-FEAnGA and [^{18}F]-FEA was also studied in CT26 cells (wild-type mouse colon adenocarcinoma cells) and CT26m β GUS cells (CT26 cells that are engineered to express β -GUS as an anchored enzyme on the outer surface of the cell membrane) (4). With [^{18}F]-FEA, a 14-fold higher amount of radioactivity accumulated in the control CT26 cells than with [^{18}F]-FEAnGA. Incubation of CT26 cells (controls) and the CT26m β GUS cells with [^{18}F]-FEAnGA showed that the latter cells had a 3-fold higher amount of radioactivity associated with the cells compared with the control cells. Radio-TLC of the growth medium of the CT26m β GUS cells showed that

20% of the $[^{18}\text{F}]\text{-FEAnGA}$ was converted to $[^{18}\text{F}]\text{-FEA}$ by the $\beta\text{-GUS}$ anchored on the membrane surface of these cells (4).

Animal Studies

Rodents

[PubMed]

A preliminary study was performed in two mice bearing CT26 and CT26 βGUS cell tumors on the right and left shoulders, respectively, to evaluate the use of $[^{18}\text{F}]\text{-FEAnGA}$ for the detection of $\beta\text{-GUS}$ expression with PET (4). The animals were injected with either $[^{18}\text{F}]\text{-FEAnGA}$ (4.4 MBq (118.8 μCi)) or $[^{18}\text{F}]\text{-FEA}$ (4.2 MBq (113.4 μCi)) through the penile vein, and a microPET scan was acquired for 60 min. At 1 h p.i., PET images of the animal injected with $[^{18}\text{F}]\text{-FEAnGA}$ showed a 2-fold higher uptake of radioactivity in the CT26 βGUS cell tumor compared with the CT26 cell control tumor. The increased uptake of radioactivity by the CT26 βGUS tumor was attributed to the production of $[^{18}\text{F}]\text{-FEA}$ from $[^{18}\text{F}]\text{-FEAnGA}$ by the $\beta\text{-GUS}$ on the surface of the CT26 βGUS cells (4). The animals injected with $[^{18}\text{F}]\text{-FEA}$ did not show any accumulation of radioactivity in the CT26 βGUS cell tumor. No blocking studies were reported. From this preliminary study, the investigators concluded that $[^{18}\text{F}]\text{-FEAnGA}$ may be used as a tracer to visualize tumors that express the $\beta\text{-GUS}$ enzyme in rodents (4).

The *ex vivo* biodistribution of $[^{18}\text{F}]\text{-FEAnGA}$ was investigated in healthy anesthetized Wistar rats ($n = 5$ animals) injected with 5.04 ± 1.80 MBq (136.08 ± 48.6 μCi) of the radiochemical through the penile vein (2). At 60 min p.i., very low radioactivity uptake was observed in the major organs of the animals. The kidneys showed an uptake of 0.53 ± 0.24 standardized uptake values (SUV), and the liver showed an uptake of 0.15 ± 0.04 SUV, indicating that the tracer was cleared rapidly from the system through the renal pathway.

The use of $[^{18}\text{F}]\text{-FEAnGA}$ with PET was evaluated for the detection of C6 cell tumors or muscular inflammation (induced with turpentine) in Wistar rats ($n = 8$ animals) (2). Two microPET scans were acquired from each animal after $[^{18}\text{F}]\text{-FEAnGA}$ injection as described above. The first scan was performed to detect small (<1.5 cm^3) and large (>1.5 cm^3) tumors at 8 days after inoculation of the C6 cells to induce the tumors. The second PET scan was performed for the detection of the tumor and inflammation at 13 days after the C6 injection. Images obtained from the first PET scan showed that there was a uniform distribution of radioactivity from $[^{18}\text{F}]\text{-FEAnGA}$ in the small tumors; however, the large tumors showed a high uptake of label only in the viable outer periphery of the lesions, whereas the non-viable parts of the large tumors had a low accumulation of the tracer. Time-activity curves of the tumors showed that the small tumors had peak accumulation of radioactivity at 1.5 min p.i. with a tracer half-life of 12 ± 3 min. The half-life of radioactivity in the viable parts of the large tumors was reported to be 24 ± 13 min, and the area under the curve (AUC) for these lesions was 1.7-fold greater than that of the

small tumors ($P = 0.05$). The PET scan at 13 days after inoculation of the C6 cells showed that the accumulation of radioactivity in the inflamed muscle (0.07 ± 0.05 SUV) was significantly higher than that observed in the normal muscle (0.04 ± 0.03 SUV; $P < 0.05$). From these studies, the investigators concluded that [^{18}F]-FEAnGA can be used to detect and understand the activity of β -GUS in cancerous tumors and inflamed tissues in rodents (2).

The use of [^{18}F]-FEAnGA with PET was evaluated in a rat model of herpes encephalitis for the detection of β -GUS activity released in the tissue during neuroinflammation (10). Male Wistar rats were infected with herpes simplex virus-1 (HSV-1) to induce herpes encephalitis in the animals ($n = 8$ rats; as controls, $n = 4$ rats), and microPET scans were acquired from the rodents after intravenous penile injection of [^{18}F]-FEAnGA as described above (10). A low uptake of radioactivity was observed in the brains of the infected and the control animals. The AUC (10–60 min p.i.) for whole brains of the HSV-1-infected animals was 2-fold higher ($P = 0.05$) than that of the control rats (AUC = 5 ± 1). Brain homogenates of the HSV-1-infected rats showed 3.4-fold higher activity of β -GUS compared with the enzyme activity in the brain homogenates of control animals (10). From this study, the investigators concluded that, although there was a low uptake of label from [^{18}F]-FEAnGA in the brain, this tracer could be used to detect increased β -GUS activity in the organ due to neuroinflammation (10).

Other Non-Primate Mammals

[PubMed]

No publication is currently available.

Non-Human Primates

[PubMed]

No publication is currently available.

Human Studies

[PubMed]

No publication is currently available.

Supplemental Information

[Disclaimers]

No information is currently available.

References

1. Cheng T.C., Roffler S.R., Tzou S.C., Chuang K.H., Su Y.C., Chuang C.H., Kao C.H., Chen C.S., Harn I.H., Liu K.Y., Cheng T.L., Leu Y.L. *An activity-based near-infrared glucuronide trapping probe for imaging beta-glucuronidase expression in deep tissues.* J Am Chem Soc. 2012;134(6):3103–10. PubMed PMID: 22239495.
2. Antunes I.F., Haisma H.J., Elsinga P.H., van Waarde A., Willemsen A.T., Dierckx R.A., de Vries E.F. *In Vivo Evaluation Of 1-o-(4-(2-fluoroethyl-carbamoyloxymethyl)-2-nitrophenyl)-o-beta-d-glucopyronurona te: A Positron Emission Tomographic Tracer For Imaging beta-glucuronidase Activity In A Tumor/inflammation Rodent Model.* Mol Imaging. 2012;11(1):77–87. PubMed PMID: 22418030.
3. Gandhi N.S., Freeman C., Parish C.R., Mancera R.L. *Computational analyses of the catalytic and heparin-binding sites and their interactions with glycosaminoglycans in glycoside hydrolase family 79 endo-beta-D-glucuronidase (heparanase).* Glycobiology. 2012;22(1):35–55. PubMed PMID: 21746763.
4. Antunes I.F., Haisma H.J., Elsinga P.H., Dierckx R.A., de Vries E.F. *Synthesis and evaluation of [18F]-FEAnGA as a PET Tracer for beta-glucuronidase activity.* Bioconjug Chem. 2010;21(5):911–20. PubMed PMID: 20415436.
5. Antunes I.F., Haisma H.J., de Vries E.F. *Tumor-specific activation of prodrugs: is there a role for nuclear medicine?* Nucl Med Commun. 2008;29(10):845–6. PubMed PMID: 18769302.
6. Huttunen K.M., Raunio H., Rautio J. *Prodrugs--from serendipity to rational design.* Pharmacol Rev. 2011;63(3):750–71. PubMed PMID: 21737530.
7. Thomas M., Clarhaut J., Tranoy-Opalinski I., Gesson J.P., Roche J., Papot S. *Synthesis and biological evaluation of glucuronide prodrugs of the histone deacetylase inhibitor CI-994 for application in selective cancer chemotherapy.* Bioorg Med Chem. 2008;16(17):8109–16. PubMed PMID: 18692397.
8. Renoux B., Legigan T., Bensalma S., Chadeneau C., Muller J.M., Papot S. *A new cycloamine glucuronide prodrug with improved kinetics of drug release.* Org Biomol Chem. 2011;9(24):8459–64. PubMed PMID: 22042246.
9. Tzou S.C., Roffler S., Chuang K.H., Yeh H.P., Kao C.H., Su Y.C., Cheng C.M., Tseng W.L., Shiea J., Harm I.H., Cheng K.W., Chen B.M., Hwang J.J., Cheng T.L., Wang H.E. *Micro-PET imaging of beta-glucuronidase activity by the hydrophobic conversion of a glucuronide probe.* Radiology. 2009;252(3):754–62. PubMed PMID: 19717754.
10. Antunes I.F., Doorduyn J., Haisma H.J., Elsinga P.H., van Waarde A., Willemsen A.T., Dierckx R.A., de Vries E.F. *18F-FEAnGA for PET of beta-Glucuronidase Activity in Neuroinflammation.* J Nucl Med. 2012;53(3):451–8. PubMed PMID: 22323774.
11. Willmann J.K., van Bruggen N., Dinkelborg L.M., Gambhir S.S. *Molecular imaging in drug development.* Nat Rev Drug Discov. 2008;7(7):591–607. PubMed PMID: 18591980.